

Vibrational and magnetic properties of crystalline CuTe_2O_5

Y. V. Lysogorskiy¹⁾, R. M. Eremina^{+,*}, T. P. Gavrilova^{+,*}, O. V. Nedopekin^{+,*}, D. A. Tayurskii^{+,×}

⁺*Institute of Physics, Kazan (Volga Region) Federal University, 420008 Kazan, Russia*

^{*}*Zavoisky Physical-Technical Institute of the RAS, 420029 Kazan, Russia*

[×]*Centre for Quantum Technologies, Kazan (Volga Region) Federal University, 420008 Kazan, Russia*

Submitted 9 October 2014

In the present work we have performed an *ab initio* calculation of vibrational properties of CuTe_2O_5 by means of density functional theory (DFT) method. One has compared calculated values with known experimental data on Raman and infrared spectroscopy in order to verify the obtained results. Lattice contribution to the heat capacity, obtained from the *ab initio* simulations was added to magnetic contribution calculated from the simple spin hamiltonian model in order to obtain total heat capacity. Obtained results are in good agreement with the experimental data. Thus, the DFT methods could complement the experimental and theoretical studying of low-dimensional magnetic systems such as CuTe_2O_5 .

DOI: 10.7868/S0370274X14220111

1. Introduction. The low-dimensional magnet CuTe_2O_5 has attracted much attention because of the dispute concerning the magnetic structure of this compound. One-dimensional magnetic structure was suggested based on ESR measurements [1, 2], while the two dimensional model was proposed from first-principles electronic structure calculations [3, 4] and heat capacity measurements [5].

In the present work we have performed an *ab initio* calculations of lattice vibrational properties of crystalline CuTe_2O_5 , and made a comparison with available experimental data on Raman and infrared (IR) spectroscopies in order to verify obtained results. On the next step, the magnetic contribution to the heat capacity, calculated from alternating spin chain model (present work) and 2D-coupled dimer model [3] were added to lattice contribution in order to obtain total heat capacity and compare with the known experimental data [5].

2. Computational details. Calculations taking into account spin-polarization effects were performed within the framework of density functional theory (DFT) with gradient-corrected exchange and correlation energy functional proposed by Perdew–Burke–Ernzerhof (PBE) [6] and projector augmented-wave method as implemented in the code VASP [7, 8] (a part of the MedeA software package [9]). The $\text{O}(2s^22p^4)$, $\text{Cu}(3d^{10}4s^1)$, and $\text{Te}(5s^25p^4)$ electrons were treated explicitly, whereas the rest were considered through the pseudopotentials. The maximum energy for plane wave

basis set was selected to be equal 400 eV. The electronic strong correlations were treated within the simplified (rotationally invariant) GGA+U approach, introduced by Dudarev et al. [10]. The Coulomb on-site repulsion parameter U for Cu d -electrons was set to 8 eV, while Hund's rule coupling (J_H) parameter was selected to be equal to 1 eV [4]. Integration over the Brillouin zone (BZ) has been performed on a Mokhorst–Pack mesh $3 \times 3 \times 3$ [11] for primitive cell during structure optimization and over Γ -point only while considering the lattice vibrations. Equilibrium geometry has been obtained after the several stages of full structure relaxation, that include optimization of atomic position, cell shape and cell volume. The phonon dispersion and density of states (DOS) were obtained by use of MedeA-PHONON module, which implements a direct approach of harmonic approximation [12]. The so called direct approach to lattice dynamics is based on the *ab initio* evaluation of forces on all atoms produced by a set of finite displacements of a few atoms within an otherwise perfect crystal. The IR and Raman spectra were calculated from the phonon frequencies at Γ -point. For the IR and Raman intensities the dielectric tensor, the Born effective charges and the Raman tensor were calculated by means of linear response calculations, also implemented in VASP [7, 8].

3. Results and discussions. *3.1. Structural properties.* The CuTe_2O_5 possesses a monoclinic structure with space group $P2_1/c$ and experimental lattice parameters $a = 6.871 \text{ \AA}$, $b = 9.322 \text{ \AA}$, $c = 7.602 \text{ \AA}$, and $\beta = 109.08^\circ$ [13]. The lattice parameters obtained after structure relaxation were $a = 6.756 \text{ \AA}$, $b = 9.302 \text{ \AA}$,

¹⁾e-mail: yura.lysogorskii@gmail.com

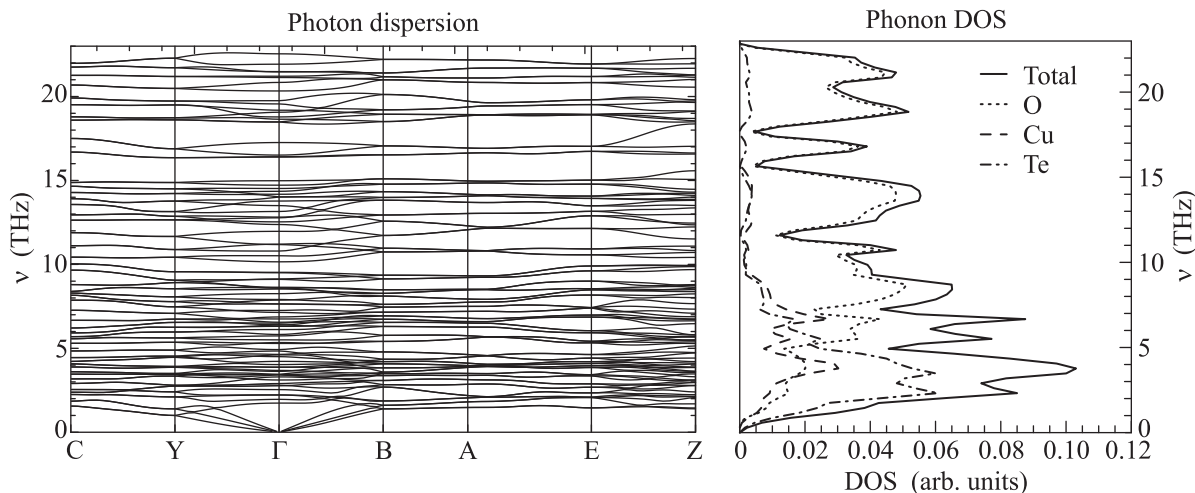


Fig. 1. Phonon dispersion and density of states, projected onto Cu, Te and O atoms for crystalline CuTe_2O_5

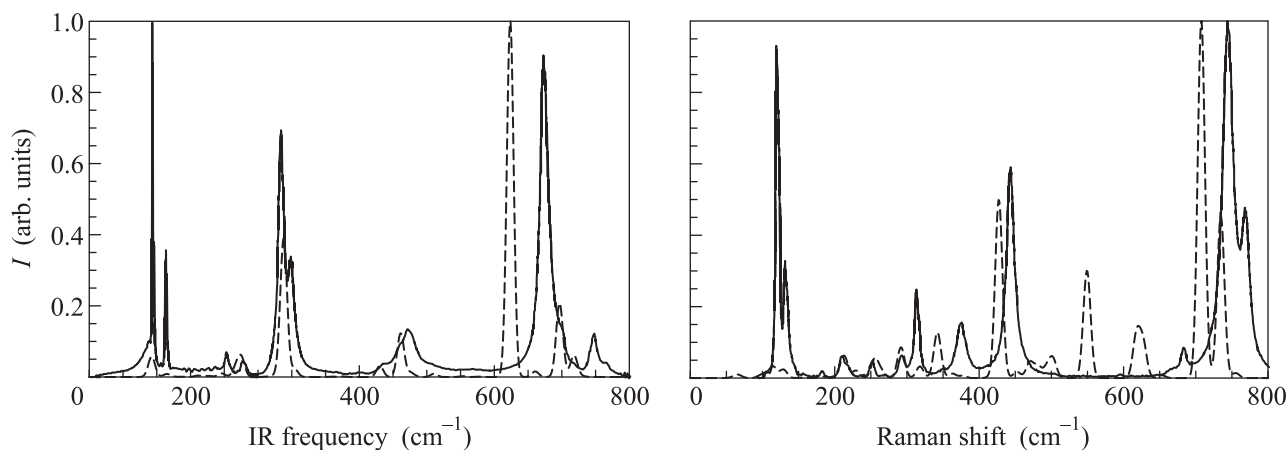


Fig. 2. Calculated (dashed lines) and experimental (solid lines) [14] spectra for IR and Raman measurements, normalized to the maximum peak intensity. See text for details

$c = 7.353 \text{ \AA}$, and $\beta = 109.08^\circ$. The calculated lattice parameters are all underestimated by 2–3%, which is a normal DFT error. Moreover the calculated values correspond to the case $T = 0 \text{ K}$, whereas the experimental ones could be larger because they were measured at finite temperature.

The magnetic moment on Cu ions was found to be $0.75 \mu_B$, which well corresponds to the value $0.79 \mu_B$ obtained previously [4]. In the previous studies the dominant antiferromagnetic interaction between Cu ions has been demonstrated [3]. We have considered two type of magnetic ordering in the Cu–Cu dimers, which realize the $P2_1$ and Pc subgroups of crystal space group $P2_1/c$. In the former case, two Cu–Cu dimers in the crystal cell are oriented antiferromagnetically, while in the latter case – ferromagnetically. The magnetic ordering with $P2_1$ symmetry has smaller energy of about 2 meV per Cu atom in comparison to Pc and was selected as a

ground state for the further *ab initio* calculations of vibrational properties.

3.2. Vibrational properties. The phonon dispersion and phonon DOS, total and decomposed for the different atom types, were calculated as described above and are presented in the Fig. 1. One can see, that at low frequencies the dominant contribution to the lattice vibrations comes from the Cu and Te atoms, whereas the vibration modes of oxygen atoms are predominantly have higher energies.

IR and Raman spectra, calculated in the present work and experimentally measured [14], are shown in the Fig. 2. The maximum peak intensities were normalized to unity, while the line width of calculated spectra was selected to be 5 cm^{-1} . The difference between peak intensities in experimental and calculated spectra can be attributed to the different orientations of crystal in experiment and calculations. However, calcu-

lated positions of peaks below 400 cm^{-1} for both IR and Raman spectra are coincide well with the experimental ones. But there is some frequency underestimation for $\nu \geq 400\text{ cm}^{-1}$ with a magnitude of about 50 cm^{-1} . The underestimation of the frequency of the stretching modes is probably due to the overestimation of the bond length, which was reported previously for example in Ref. [15] for Te–O stretching modes above 500 cm^{-1} , where the *ab initio* study of the vibrational properties of crystalline TeO_2 was performed.

Nevertheless, one can assume that vibrations at frequencies above 400 cm^{-1} become active only at temperatures of about 500 K and their contribution to the heat capacity in the temperature range $10\text{--}100\text{ K}$ is negligible.

3.3. Heat capacity. Lattice contribution. We assume that the total heat capacity originates from two different contributions, a lattice (phonon) contribution C_{latt} due to acoustic and optical phonons and a magnetic contribution C_{magn} determined by the thermal population of excited spin states.

In order to calculate the phonon contribution to the heat capacity of CuTe_2O_5 we have used approach based on the harmonic approximation, so that heat capacity could be found as [16]

$$C(T) = dk_{\text{B}} \int_0^{\infty} g(\omega) \left(\frac{\hbar\omega}{2k_{\text{B}}T} \right)^2 \frac{\exp(\hbar\omega/k_{\text{B}}T)}{[\exp(\hbar\omega/k_{\text{B}}T) - 1]^2} d\omega, \quad (1)$$

where d is the number of degrees of freedom in the unit cell, $g(\omega)$ is a total phonon DOS, which is shown in the Fig. 1, \hbar and k_{B} are the Planck and Boltzmann constants, and T is temperature.

The lattice contribution to the heat capacity calculated from the harmonic approximation is shown in the Fig. 3a and compared to the experimentally measured total heat capacity from Ref. [5]. The calculated values are higher than the experimental ones at high temperatures $T > 150\text{ K}$, and it could be explained by the underestimation of calculated vibration frequencies above 400 cm^{-1} that leads to the overestimation of heat capacity.

It is well known, that at low temperatures the lattice contribution to the heat capacity demonstrates the cubic dependence on the temperature. Thus all calculated and experimental data divided by T^3 are plotted as a function of T in the Fig. 3b. It can be seen, that at the temperatures below 15 K the calculated lattice contribution to the heat capacity obeys this law, i.e. proportional to the T^3 . On the other hand, there is peak on the experimental heat capacity curve. This peak could

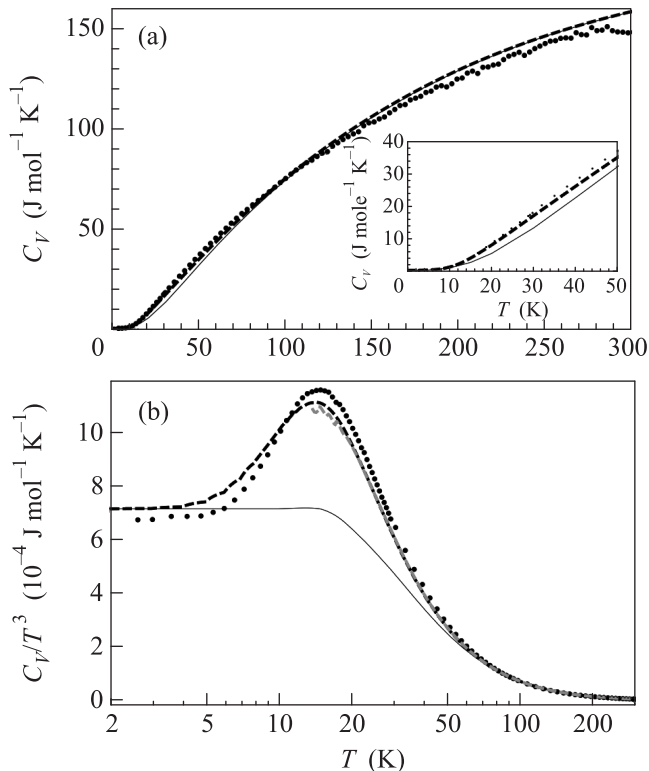


Fig. 3. Heat capacity C_V (a) and heat capacity divided by T^3 (b) for CuTe_2O_5 as a function of temperature: experimental data (dots), lattice contribution (black solid line), sum of lattice and magnetic contributions (present work, black dashed line), and sum of lattice contribution with magnetic contribution, calculated with 2D-coupled dimer model [3] (gray dashed line)

be associated with the magnetic contribution C_{magn} to the heat capacity, described in the section below.

3.4. Magnetic contribution. Evidently, the magnetic contribution to the heat capacity is small compared to the lattice contribution and a non-magnetic reference material is not available in the case of CuTe_2O_5 . Therefore, a straightforward experimental method to unambiguously extract the magnetic contribution from the experimental data cannot be realized.

At the same time the magnetic contribution to the heat capacity of the crystal containing the magnetic ions can be calculated theoretically as

$$C_{\text{magn}} = -T \frac{\partial^2 F}{\partial T^2}, \quad (2)$$

where T is temperature, F is the Helmholtz free energy

$$F = -T \ln \sum \exp(-E_n/T), \quad (3)$$

where E_n – energy levels of the considered spin system. The energy levels of the spin system depend on the ex-

ternal magnetic field and can be described by the spin-Hamiltonian. To calculate the magnetic contribution to the heat capacity for CuTe_2O_5 we used the following spin Hamiltonian for alternating spin chain of ten spins

$$H = \sum_{i=1}^5 J_1(S_{2i-1} \cdot S_{2i}) + J_2(S_{2i} \cdot S_{2i+1}) + g\beta H_z S_{z,i}, \quad (4)$$

where J_1 and J_2 describe the isotropic exchange interaction between spin S_{2i} and its nearest neighbours S_{2i+1} and S_{2i-1} , the last term describes the interaction of all spins with the applied magnetic field H .

In order to obtain these parameters, one can make a fitting of magnetization M and magnetic susceptibility χ of CuTe_2O_5 to the experimental data. Using above presented Eqs. (3) and (4) one can calculate these quantities as

$$M = -\frac{\partial F}{\partial H}, \quad (5)$$

$$\chi = \frac{\partial^2 F}{\partial H^2}, \quad (6)$$

where F is the Helmholtz free energy defined by Eq. (3). In the case of CuTe_2O_5 the values of isotropic exchange interactions are $J_1 = 93.3\text{ K}$ and $J_2 = 40.7\text{ K}$ as determined from susceptibility and ESR data [1, 2, 17]. The theoretically calculated magnetization for the aforementioned values of isotropic exchange interactions J_1 and J_2 for different values of external magnetic field is presented in the Fig. 4a. It could be seen that magnetization $M(T)$ at $H = 12.7\text{ T}$ is in good agreement with experimentally measured data from Ref. [5]. The temperature dependence of the magnetic susceptibility $\chi(T)$ for $H = 0.1\text{ T}$, also coincides with experimental data from Ref. [17] (Fig. 4b). So, one can conclude, that present model should describe the magnetic subsystem of CuTe_2O_5 well.

In the Fig. 5 the magnetic contribution to the heat capacity for different values of the external magnetic fields is depicted.

We have added the magnetic contribution to the heat capacity C_{magn} to the lattice contribution C_{latt} , obtained in Sec 3.3 and have compared the obtained result with experimental data [5], see Fig. 3. The sum of lattice contribution and magnetic contribution obtained from 2D-coupled dimer model [3] is also shown for comparison. The agreement between theoretical and experimental results is good enough, but there is small underestimation of heat capacity by both theoretical model. Ref. [3] is slightly lower than from the model considered in present work. One can suggest at least two possible explanations of this discrepancy: (i) additional contributions to the magnetic heat capacity; (ii) presence of

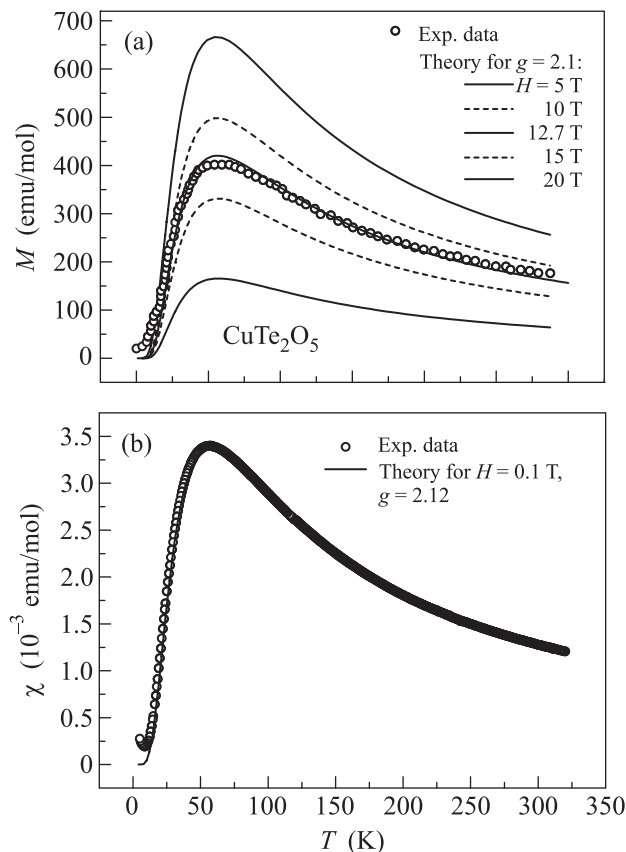


Fig. 4. Theoretically predicted temperature dependence of the magnetization (a) and magnetic susceptibility (b) of CuTe_2O_5 for different values of the external magnetic field H . Open circles correspond to the experimental data (see text)

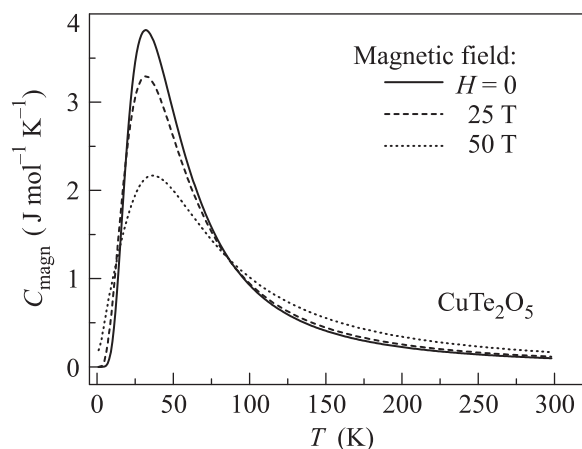


Fig. 5. Theoretically predicted temperature dependence of the magnetic contribution to the heat capacity of CuTe_2O_5 for different values of the external magnetic field H

impurities in the sample which affect the heat capacity measured experimentally.

4. Conclusion. In conclusion, the low-dimensional magnetic systems are interesting for theoretical and experimental considerations. But the theoretical calculations for such systems should be performed with a high degree of accuracy, that is achieved in the present time by using the DFT method. In our opinion, the DFT methods is suitable for calculating the physical properties of the magnetic systems, such as the lattice heat capacity, Raman and IR spectra, etc. However, to obtain the good agreement between the theoretical and experimental results, especially at low temperatures, it is necessary to consider the contribution of the magnetic subsystem, as shown for CuTe_2O_5 in this paper. Thus, the lattice heat capacity in combination with the theoretically calculated magnetic contribution is consistent with experimental data at low temperature region, where the magnetic contribution is most important.

The work is performed according to the Russian Government Program of Competitive Growth of Kazan Federal University.

1. R. M. Eremina, T. P. Gavrilova, H. Krug von Nidda, A. Pimenov, J. Deisenhofer, and A. Loidl, *Phys. Sol. State* **50**, 283 (2008).
2. T. P. Gavrilova, R. M. Eremina, H. Krug von Nidda, J. Deisenhofer, and A. Loidl, *J. of Optoelectron. and Adv. Mat.* **10**, 1655 (2008).
3. H. Das, T. Saha-Dasgupta, C. Gros, and R. Valentí, *Phys. Rev. B* **77**, 224437 (2008).
4. A. Ushakov and S. Streltsov, *J. Phys.: Cond. Matt.* **21**, 305501 (2009).
5. R. Eremina, T. Gavrilova, A. Günther, Z. Wang, R. Lortz, M. Johnsson, H. Berger, H. Krug von Nidda, J. Deisenhofer, and A. Loidl, *Eur. Phys. J. B* **84**, 391 (2011).
6. J. P. Perdew, K. Burke, and M. Ernzerhof, *Phys. Rev. Lett* **77**, 3865 (1996).
7. G. Kresse and J. Furthmüller, *Phys. Rev. B* **54**, 11169 (1996).
8. G. Kresse and D. Joubert, *Phys. Rev. B* **59**, 1758 (1999).
9. *Materials Design 2013 Medea Version 2.14* (Angel Fire, NM: Materials Design).
10. S. L. Dudarev, G. A. Botton, S. Y. Savrasov, C. J. Humphreys, and A. P. Sutton, *Phys. Rev. B* **57**, 1505 (1998).
11. J. P. H. Monkhorst, *Phys. Rev. B* **13**, 5188 (1976).
12. K. Parlinski, Z. Li, and Y. Kawazoe, *Phys. Rev. Lett.* **78**, 4063 (1997).
13. K. Hanke, V. Kupcik, and O. Lindqvist, *Acta Crystallogr. Sect. B: Struct. Crystallogr. Cryst. Chem.* **29**, 963 (1973).
14. L. Agazzi, *Vibrational properties of CuTe_2O_5* , *PhD thesis* (2006/2007).
15. M. Ceriotti, F. Pietrucci, and M. Bernasconi, *Phys. Rev. B* **73**, 104304 (2006).
16. C. Kittel and P. McEuen, *Introduction to Solid State Physics*, Wiley, N.Y. (1976), v. 8.
17. J. Deisenhofer, R. M. Eremina, A. Pimenov, T. Gavrilova, H. Berger, M. Johnsson, P. Lemmens, H. Krug von Nidda, A. Loidl, K.-S. Lee, and M.-H. Whangbo, *Phys. Rev. B* **74**, 174421 (2006).